



A Design Method of Multi-link Cable Driven Robots Considering the Rigid Structure Design and Cable Routing

Yaoxin Guo^(✉) and Darwin Lau

The Chinese University of Hong Kong, Sha Tin, Hong Kong
yxguo@mae.cuhk.edu.hk, darwinlau@cuhk.edu.hk

Abstract. Multi-link cable driven robots (MCDRs) have attracted much attention in recent years and have been widely used in complex working environments due to their inherent high compliance and flexibility. Although lots of work have studied on the cable routing arrangement of MCDRs, because of the highly coupled relationship between the rigid structure and cable routing, to improve the overall performance of the robot, it is necessary but challenging to take the rigid structure into account. In this paper, we propose a co-design method for MCDRs, which is based on configuration planning with target reachability and structure design with cable routing arrangement according to wrench feasibility. The complete set of design variables can be determined by applying the proposed co-design method for both rigid-links and the cable routing arrangement. Furthermore, the example results for a planar MCDR demonstrate the rationality and applicability of the proposed method.

1 Introduction

Multi-link cable driven robots (MCDRs) are a type of multi-joints serial robot actuated by cables [1]. This type of robot has attracted increasingly more attention in recent years owing to its many advantages, such as high compliance and dexterity, low self-weight compared with traditional serial rigid robots, and large rotational workspace. Due to these advantages, MCDRs have allowed a range of exciting applications, such as the hazardous material industry [2] and in-pipe inspection robot [3].

For MCDRs, both the cable routing arrangement, that means the number of cables and the cable attachment of each cable on every rigid-link, and the dimensions of rigid-links are vital to the robot's performance [4]. Most importantly, all the design variables that can fully define the whole MCDR significantly influence the robot's Jacobian matrix [5], and other robot properties such as the workspace, required maximum cable forces and stiffness [6]. However, determining the complete set of design variables is challenging due to the highly non-linear and complex relationship between the performance of MCDRs and the design variables.

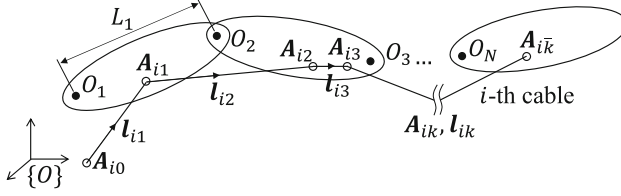


Fig. 1. General Model of MCDRs.

Most existing MCDR designs only focus on studying cable routing schemes, and many different routing schemes have been proposed. The most intuitive one is a directly driven routing scheme in that the cables directly connect one rigid-link to the base [7], thus, the number of cables is relatively large. Then, the co-sharing routing scheme is put forward, which can be divided into two categories as *external co-sharing routing scheme* and *internal co-sharing routing scheme* [8]. The difference between these two schemes is *internal scheme* will have the cable routing inside one specific rigid-link. Thus, different cable routing schemes can be considered for different required performances, such as tension reduction [9] and workspace amplification [10].

In addition to the optimal cable routing scheme, the design of rigid-links also has a crucial impact on the performance of MCDRs. For example, based on specific tasks, if the number of rigid-links is over-required, it will not only increase the redundancy and complexity of the entire MCDR, but also increase the self-weight and inertia, which will weaken the advantages of using this type of robot. Thus, the complete design method of MCDRs, which includes both the cable routing arrangement and the design of rigid-links, is needed to be studied in depth. However, the complete design problem is challenging due to the highly coupled relationship between rigid-links and cable routing schemes.

In this paper, a novel co-design method of configuration planning and structure design is proposed to determine the entire set of design variables for MCDRs that are both for rigid-links and cable routing arrangement, which is a task-specific design method that considers reachability and wrench feasibility. Finally, a planar MCDR is used as an example to illustrate the rationality and applicability of the proposed method.

2 Background of MCDRs

Figure 1 shows a general multi-link cable driven robot (MCDR) that actuated by m cables with $i = 1, \dots, m$, and is comprised of N rigid-links that $j = 1, \dots, N$. Then, the attachment point (both fixed point and go-through point) of i -th cable on k -th segment (total $\bar{k} \geq N$) is denoted by A_{ik} . The kinematics of the cable vector can be expressed as

$$l_{ik} = A_{ik}^o(q) - A_{i(k-1)}^o(q) \quad (1)$$

where $\mathbf{q} = [\mathbf{q}_1^T, \dots, \mathbf{q}_N^T]^T$ is the whole-body configuration, which depends on the corresponding joint type. Moreover, $A_{ik}^o(\mathbf{q})$ represents the corresponding cable attachment point in global frame, and \mathbf{l}_{ik} is the cable vector through k -th segment of i -th cable. Then, the length of i -th cable l_i and the corresponding $\dot{\mathbf{l}}_i$ are expressed as

$$\begin{aligned} l_i &= \sum_{j=1}^{\bar{k}} \|\mathbf{l}_{ik}\| \\ \dot{\mathbf{l}}_i &= \sum_{k=1}^{\bar{k}} \dot{\mathbf{l}}_{ik} = \sum_{k=1}^{\bar{k}} \hat{\mathbf{l}}_{ik} \cdot \dot{\mathbf{l}}_{ik} \end{aligned} \quad (2)$$

Hence, differential kinematics of MCDRs can be concluded in the generalized coordinate that $\dot{\mathbf{l}} = J(\mathbf{q}) \cdot \dot{\mathbf{q}}$, with $J(\mathbf{q})$ is the Jacobian matrix. Denoting J_i as i -th row of the Jacobian matrix, which can be obtained by solving Eqs. (1) and (2) that $\dot{\mathbf{l}}_i = J_i \cdot \dot{\mathbf{q}}$. Based on the kineto-static duality of robotics, the static equilibrium equation of MCDRs is

$$J^T(\mathbf{q}) \cdot \mathbf{f} = \boldsymbol{\tau}(\mathbf{q}) \quad (3)$$

where $\mathbf{f} = [f_1, \dots, f_m]^T$ is the cable force vector such that $\underline{\mathbf{f}} \preceq \mathbf{f} \preceq \bar{\mathbf{f}}$, and $\boldsymbol{\tau}(\mathbf{q})$ is the generalized external force vector.

It is well known that the overall performance of MCDRs can be analyzed through the analysis of the Jacobian matrix. However, the Jacobian matrix of MCDRs depends on not only the configuration \mathbf{q} but also structure parameters, such as the number of cables and the length of each rigid-link. Thus, it is crucial to consider the performance of the MCDR during the design phase.

3 Problem Formulation

In order to design a MCDR according to specific task requirements, the set of design variables considered in this work is defined as $\mathcal{D} = \{N, L_j, m, \mathbf{A}_{ij}, \bar{f}_i\}$, where N is the total number of rigid-links and m is the total number of cables, while L_j is the length of rigid-link j , $j = 1, \dots, N$, also \mathbf{A}_{ik} and \bar{f}_i are the cable attachment point on each segment k of cable i , $i = 1, \dots, m$ and the corresponding cable force limit, respectively.

The first two kinds of variables are rigid-link parameters, while the latter three can decide the cable arrangement and guide motor selection. The whole set of design variables is necessary to be determined before actual processing. The proposed design method is based on specific task requirements, and the design inputs are:

- \mathbf{S}, \mathbf{T} are the desired start and end position of the tip, respectively;
- \mathbf{w}_d is the required wrench vector on the tip of the MCDR; and
- \mathcal{O} represents obstacles that the MCDR needs to avoid during work processes.

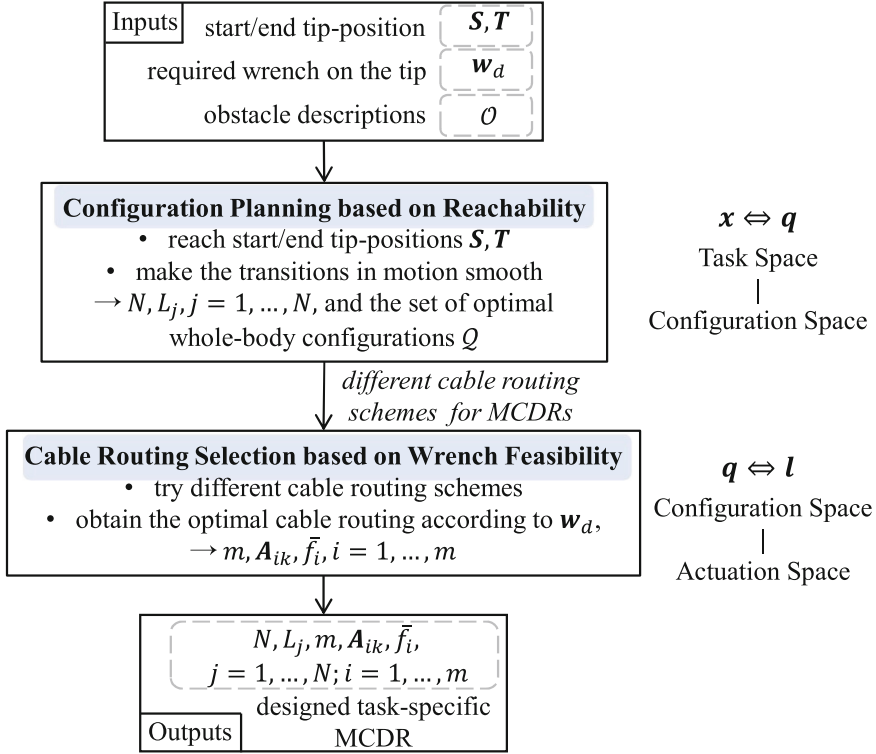


Fig. 2. Proposed Co-design Concept for MCDRs.

As shown in Fig. 2, the proposed co-design method of MCDRs with configuration planning and structure design includes two steps.

1. Configuration planning based on reachability: To achieve the desired tip-positions (\mathbf{S} and \mathbf{T}) while avoiding the obstacles (\mathcal{O}), N and each L_j must satisfy some conditions. In this work, the rapidly exploring random tree (RRT) method is used to decide N and $L_j, j = 1, \dots, N$, which will be discussed in Sect. 4.1 and Sect. 4.2. Then, to enable smooth transitions of the tip from \mathbf{S} to \mathbf{T} , a set of whole-body configurations \mathcal{Q} will be derived in Sect. 4.3. Moreover, the first step is mainly focus on the design of rigid-links.
2. Cable routing selection based on wrench feasibility: Denoting the cable routing arrangements of MCDRs by $\{m, \mathbf{A}_{ik}, \bar{f}_i\}$, and continuing on the result of the first step, the optimal cable routing scheme can be determined through cable force attributes according to the desired wrench \mathbf{w}_d at each configuration $\mathbf{q} \in \mathcal{Q}$. The second step will be explained in Sect. 5.

By applying the proposed design method, the output will be the entire set of design variables \mathcal{D} .

4 Configuration Planning Based on Reachability

It is well known that rigid-link structure plays a dominant role in the reachability of MCDRs for specific targets of the tip, and reachability represents one of the conditions that MCDRs must match in practical projects. Thus, in this section, the design variables of rigid-links N and $L_j, j = 1, \dots, N$ will be decided first to achieve the desired tip positions. Furthermore, through the tip-transition from S to T , a set of whole-body configuration \mathcal{Q} will yield.

4.1 RRT Algorithm

The proposed design method uses the RRT planning algorithm with a fixed search step for finding the necessary number of rigid-links N of the MCDR based on reachability while avoiding obstacles. While, as shown in Fig. 3, nodes in the RRT concept represent the corresponding joints of MCDRs in this work, which is related to N , and the fixed search step can be treated as the length L_j of the j -th rigid-link. Consequently, the line-segment between two nodes is shown as the corresponding rigid-link.

The basic concept of the RRT algorithm with referring to [11], the initial search tree \mathcal{T} is generated first according to the known obstacles, and \mathcal{V} is the selection set of feasible samples. Then the nearest node (joint of the MCDR) $\mathbf{x}_{nearest} \in \mathcal{V}$ to the samples $\mathbf{x}_{sample} \in \mathcal{T}$ can be selected. Thus, by applying the fixed search step (rigid-link length) L , the new node can be assigned as

$$\mathbf{x}_{new} = \mathbf{x}_{nearest} + L \cdot \frac{\mathbf{x}_{sample} - \mathbf{x}_{nearest}}{\|\mathbf{x}_{sample} - \mathbf{x}_{nearest}\|} \quad (4)$$

It is necessary to check the collision situation with obstacles and line-segment $\overline{\mathbf{x}_{nearest}\mathbf{x}_{new}}$, and if it is collision free, the new node \mathbf{x}_{new} can be added into \mathcal{V} which is connected to the corresponding $\mathbf{x}_{nearest}$.

Furthermore, if the distance between \mathbf{x}_{new} and T_{target} (like the desired tip-position S and T in this work) is no more than the fixed search step L that $|\mathbf{x}_{new}T_{target}| \leq L$, the search process will end. The output result will be the node set \mathcal{V} with the information of node-connections with fixed search step.

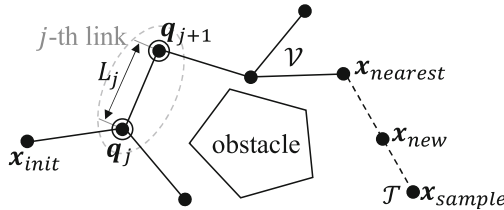


Fig. 3. Illustration of RRT Algorithm with Fixed Search Step.

4.2 Adjustment of the Length of Rigid-Links

Because the fixed search step (rigid-link length) is considered during the RRT search process, except the length of the last rigid-link ($|\mathbf{x}_{new}T_{target}| \leq L$), all other rigid-links are of equal length to the fixed L that $L_1 = L_2 = \dots = L_{N-1} = L$. However, for the length of the last rigid-link L_N , it may be different for different desired tip-position, thus, the adjustment process of L_N needs to be considered.

By applying the RRT with a fixed search step based on the start/end tip-positions \mathbf{S} and \mathbf{T} , the length of the last rigid-link is denoted as $L_s = |\mathbf{x}_{N-1}^s \mathbf{S}|$ and $L_t = |\mathbf{x}_{N-1}^t \mathbf{T}|$, separately. In order to make the designed MCDR has lower self-weight and lower inertia, by regulating the whole-body configuration slightly, it is possible to make the length of the last rigid-link as that

$$L_N = \min(L_s, L_t) \quad (5)$$

Thus, the number of rigid-links of the MCDR with the corresponding rigid-link length $(N, L_j, j = 1, \dots, N)$ are decided based on reachability.

4.3 Whole-Body Configuration Planning

Furthermore, as shown in Fig. 3, the corresponding whole-body configuration is known simultaneously to achieve the desired tip position with the designed parameters of rigid-links. For the start tip-position, the obtained configuration is denoted as $\mathbf{q}^S = [\mathbf{q}_{S1}^T, \dots, \mathbf{q}_{SN}^T]^T$, while, \mathbf{q}^T is for the end tip-position.

To make a smooth transition of all N joints to meet the tip-position change from \mathbf{S} to \mathbf{T} , in this work, we do whole-body configuration planning by discretely interpolating each joint angle. Thus, to interpolate for \bar{k} steps, we have

$$\mathbf{q}^k = \mathbf{q}^S + \frac{k}{\bar{k}} \cdot (\mathbf{q}^T - \mathbf{q}^S), \quad k = 1, \dots, \bar{k} - 1 \quad (6)$$

Then, a set of whole-body configurations to make the tip transfer from \mathbf{S} to \mathbf{T} will be decided as $\mathcal{Q} = \{\mathbf{q}^S, \mathbf{q}^1, \dots, \mathbf{q}^{\bar{k}-1}, \mathbf{q}^T\}$, and it will be used for the future configuration-based design of the cable routing.

5 Cable Routing Selection Based on Wrench Feasibility

The cable routing arrangement of MCDRs includes the number of cables m , the cable attachment point \mathbf{A}_{ik} which is for i -th cable on k -th segment with $i = 1, \dots, m$, and the corresponding cable force limit f_i . It is known that the cable routing arrangement has a decisive effect on the overall performance of MCDRs through the influence of the Jacobian matrix.

Besides reachability, wrench feasibility based on the desired external wrench is another condition MCDRs must meet in practical projects. Thus, according to the static equilibrium in Eq. (3), it is vital to design the cable routing arrangement to make the MCDR wrench feasible.

5.1 Heuristic-Based Cable Routing Selection for MCDRs

Drawing on the heuristic-based design idea of cable driven parallel robots (CDPRs) as in [12], the heuristic-based selection of optimal cable routing scheme is used in this work. First, the heuristic cable routing scheme is not a definite cable routing arrangement but a general scheme to produce the cable routing arrangement for different requirements, which is explained in detail in [12]. Moreover, a library of heuristic cable routing schemes for MCDRs should be generated in advance based on previous experience and analysis.

Thus, the task-specific preliminary set of heuristic cable routing schemes can be picked out by designers after the rough selection process. Then, different cable routing arrangements can be derived by applying the preliminary set of heuristic cable routing schemes. After that, the final optimal cable routing arrangement will be determined through the evaluation simulations and results analysis.

5.2 Optimal Cable Routing Arrangement

While achieving the whole-body configuration as planned in Sect. 4.3, to satisfy the wrench requirement for each time-step, in this work, the evaluation for selecting the optimal cable routing arrangement is the performance of cable forces based on the required wrench vector \mathbf{w}_d .

First, the minimum norm of cable force vector is denoted as one performance indicator that

$$\begin{aligned} & \min \|\mathbf{f}\|_2 \\ & \text{s.t. } J^T(\mathbf{q}) \cdot \mathbf{f} = \boldsymbol{\tau} \\ & \mathbf{f} \succeq \mathbf{0} \end{aligned} \quad (7)$$

where $\boldsymbol{\tau}$ is the projection of the desired wrench vector \mathbf{w}_d from task space onto generalized configuration space.

In addition, since it takes into account the smooth transition of all joints of the MCDR, the change in cable forces during the movement should be the other evaluate indicator. For the change in t and $t + 1$ time-step, that

$$\begin{aligned} & \min \|\mathbf{f}^{t+1} - \mathbf{f}^t\|_2 \\ & \text{s.t. } J^T(\mathbf{q}^{t+1}) \cdot \mathbf{f}^{t+1} = J^T(\mathbf{q}^t) \cdot \mathbf{f}^t = \boldsymbol{\tau} \\ & \mathbf{f}^{t+1}, \mathbf{f}^t \succeq \mathbf{0} \\ & \mathbf{q}^{t+1}, \mathbf{q}^t \in \mathcal{Q} \end{aligned} \quad (8)$$

Furthermore, the upper limit of cable force can be decided as

$$\bar{f}_i \geq \max\{f_i(\mathbf{q}^t), \forall \mathbf{q}^t \in \mathcal{Q}\} \quad (9)$$

Finally, the optimal cable routing arrangement $(m, \mathbf{A}_{ik}, \bar{f}_i, i = 1, \dots, m)$ can be determined through the evaluation simulations and results analysis process. When the whole design of the proposed design method for MCDRs is finished, the output results are the complete set of design variables that $\mathcal{D} = \{N, L_j, m, \mathbf{A}_{ik}, \bar{f}_i\}$, with $j = 1, \dots, N, i = 1, \dots, m$.

6 Example and Results

This section uses a planar MCDR as an example to demonstrate the proposed co-design method for MCDRs. The task requirements (\mathbf{S} , \mathbf{T} , \mathcal{O} , and $\boldsymbol{\tau}$ which is projected from \mathbf{w}_d) are shown in Fig. 4. In the end, the set of design variables \mathcal{D} will be given with the result analysis. The units of length and force are *cm* and *N*, respectively. For brevity, the units are omitted below.

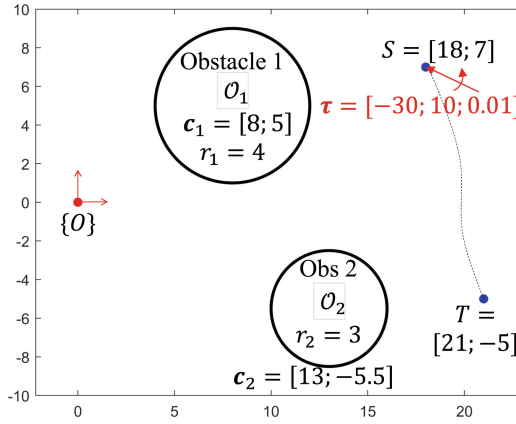


Fig. 4. Design Inputs for the Example.

6.1 Configuration Planning Based on Reachability

The first step of the proposed design method is to find a fair number of rigid-links with the corresponding length for achieving the desired tip positions.

By denoting the fixed search step as $L = 9$, the result is shown in Fig. 5. The necessary number of rigid-links is the same as $N_1 = N_2 = 3$, then we can determine the designed number of rigid-links as $N = 3$. For the length of each rigid-link, as we explained before, except for the last rigid-link length, the others are the same as the fixed search step that $L_1 = L_2 = L = 9$. However, the length of the last rigid-link differs from $L_3^S = 7.495$ and $L_3^T = 7.927$.

Thus, by applying Eq. (5), the design last rigid-link length is given as $L_3 = \min(L_3^S, L_3^T)$. In order to make the manufacturing easier, we take the approximation that $L_3 = 7.5$. After adjusting the length of rigid-links, the whole-body configurations \mathbf{q}^S and \mathbf{q}^T that are related to the desired start/end tip-positions are also decided, which is shown in Fig. 6(a).

By following Eq. (6) to interpolate $\bar{k} = 5$ steps between \mathbf{q}^S and \mathbf{q}^T , as in Fig. 6(b), the set of whole-body configurations can be obtained as

$$\mathcal{Q} = \begin{bmatrix} -37.11 & -33.52 & -29.93 & -26.34 & -22.75 & -19.16 \\ 88.59 & 79.98 & 71.37 & 62.76 & 54.16 & 45.55 \\ -5.56 & -20.47 & -35.39 & -50.30 & -65.21 & -80.13 \end{bmatrix}$$

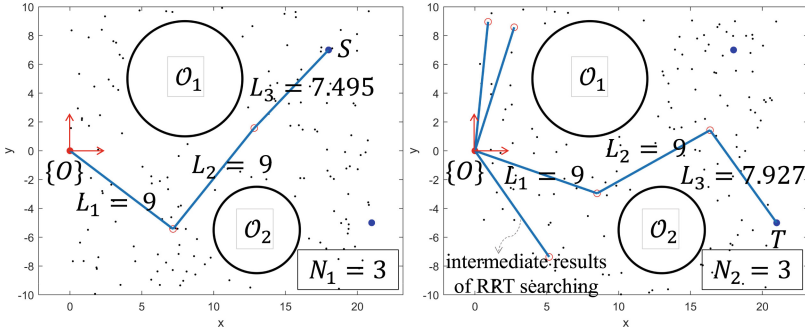


Fig. 5. Result of the RRT-planning Step with $L = 9$.

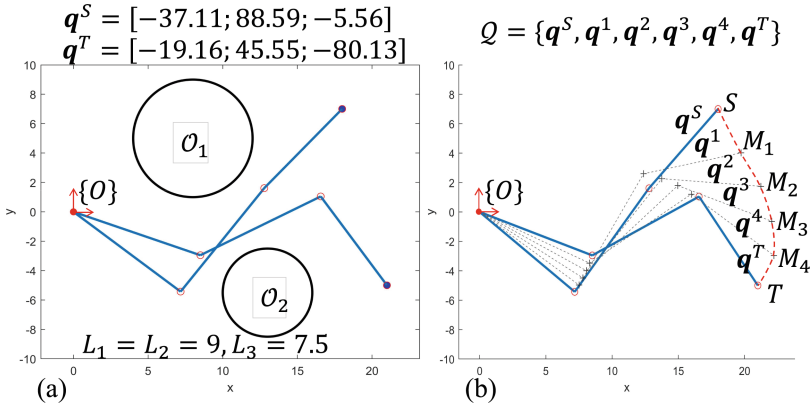


Fig. 6. (a) Designed Length in (cm) of Rigid-links based on Desired Poses Reachability with Corresponding Whole-body Configurations in degree ($^{\circ}$). (b) Planning Result of the Whole-body Configuration.

After the first step of the proposed design method, the parameters of designed rigid-links ($N = 3, L_1 = L_2 = 9$ and $L_3 = 7.5$) for the MCDR and the set of whole-body configurations Q are decided.

6.2 Cable Routing Selection Based on Wrench Feasibility

As discussed in Sect. 5.1 and [12], the generation of the library of heuristic cable routing schemes for MCDRs and selection of the preliminary set of heuristic cable routing schemes are highly depend on the experience of designers. Thus, those parts will not be expanded in detail in this example, however, Fig. 7 shows the different resulting cable routing arrangements by applying different preliminary cable routing schemes.

Figure 7(a) shows the *directly driven routing scheme*, which represents each joint is driven independently by two cables, and total 6 cables are needed.

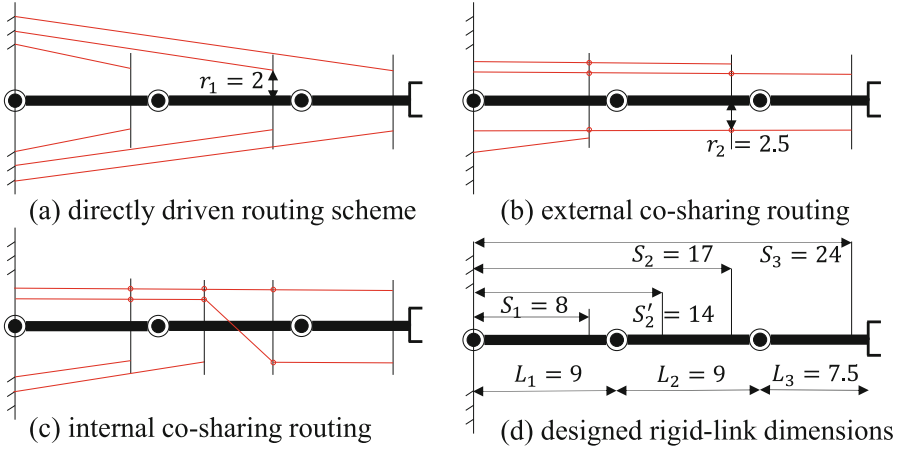


Fig. 7. A Simple Illustration of Different Cable Routing Arrangements as in (a)–(c) with Red-circles Means Where Cables Go Through, and (d) is the Designed Dimensions from the Previous Steps.

Figure 7(b) and (c) are related to *external co-sharing routing scheme* and *internal co-sharing routing scheme*, respectively, and both need 4 cables. By applying different cable routing schemes on a specific task, different cable routing arrangements containing m and A_{ik} are decided as in Fig. 7. Based on the configurations in \mathcal{Q} , to make the designed MCDR satisfies wrench feasibility for the desired external wrench w_d on the tip, the optimal cable routing arrangement can be determined through two performance indicators defined in Sect. 5.2.

First, the required maximum cable force is calculated by Eq. (7) and Eq. (9), and the results of different cable routing arrangements can be seen in Fig. 8. It shows that wrench infeasible configurations exist for *directly driven routing scheme*. Then, although *internal co-sharing routing scheme* has the smaller

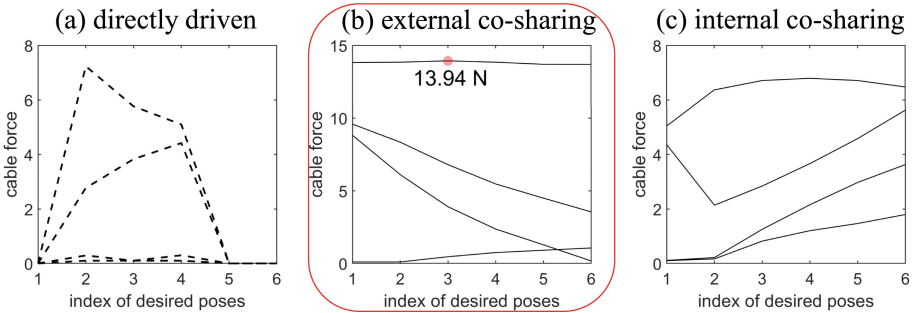


Fig. 8. Maximum Cable Force for Each Desired Pose in \mathcal{Q} based on Different Cable Routing Arrangements.

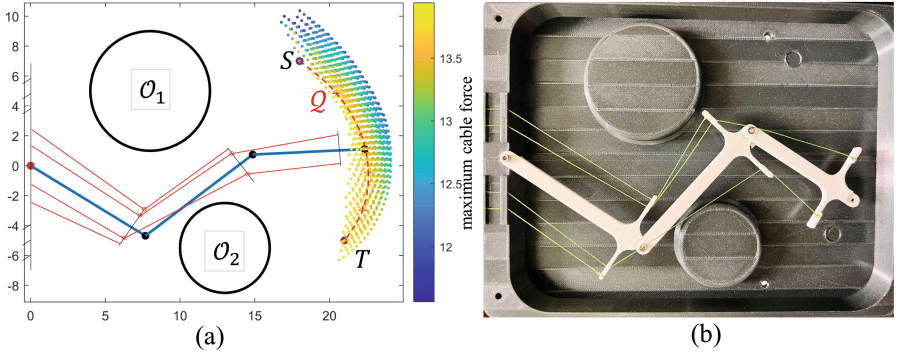


Fig. 9. (a) Combined Wrench Feasible and Collision Free Workspace of the Designed MCDR with the Joint Limits. The Colorbar Shows the Maximum Cable Force. (b) Hardware Setup of the Designed MCDR.

required cable force to meet wrench feasibility, *external co-sharing routing scheme* is smoother in the changes of cable force.

Then, the second performance indicator expressed in Eq. (8) needs to be considered together due to the maximum cable force (13.94 N) that is required for *external co-sharing routing scheme* is acceptable. The smoother change in cable force is the most important in practical applications, thus, the optimal cable arrangement is decided as the arrangement derived by *external co-sharing routing scheme*.

Finally, the complete set of design variables \mathcal{D} is derived that $N = 3$, $L_1 = L_2 = 9$, $L_3 = 7.5$, $m = 4$, and in local frame of each rigid-link that

$$\text{cable 1: } \mathbf{A}_{11} = [0, -3]^T \quad \mathbf{A}_{12} = [8, -2.5]^T \quad \bar{f}_1 = 13.94$$

$$\text{cable 2: } \mathbf{A}_{21} = [0, 3]^T \quad \mathbf{A}_{22} = [8, 2.5]^T \quad \mathbf{A}_{23} = [8, 2.5]^T \quad \bar{f}_2 = 1.07$$

$$\text{cable 3: } \mathbf{A}_{31} = [0, 2]^T \quad \mathbf{A}_{32} = [8, 2]^T \quad \mathbf{A}_{33} = [8, 2]^T \quad \mathbf{A}_{34} = [6, 2]^T \quad \bar{f}_3 = 9.59$$

$$\text{cable 4: } \mathbf{A}_{41} = [0, -2]^T \quad \mathbf{A}_{42} = [8, -2]^T \quad \mathbf{A}_{43} = [8, -2]^T \quad \mathbf{A}_{44} = [6, -2]^T \quad \bar{f}_4 = 8.82$$

The designed MCDR is shown in Fig. 9(a), and the hardware setup is in Fig. 9(b). It shows that the designed MCDR has the capability to meet the reachability and wrench feasibility by following the expected configurations.

7 Conclusion and Future Works

In this work, we put forward a new concept for MCDRs: reachability guides the design of rigid-links for MCDRs, and wrench feasibility will determine the optimal cable routing arrangement by considering two evaluate indicators about cable forces. Furthermore, all design variables can be derived through the proposed co-design method. For future works, some crucial points will be considered, such as the cable interference with both obstacles and rigid-links, the configuration singularity and friction analysis in motion.

Acknowledgements. The work was supported by the Research Grants Council (General Research Fund Reference No. 14203921) and the Innovation and Technology Commission (Innovation and Technology Support Programme Reference No. ITS/347/19FP).

References

1. Mustafa, S.K., Agrawal, S.K.: On the force-closure analysis of n-DOF cable-driven open chains based on reciprocal screw theory. *IEEE Trans. Robot.* **28**(1), 22–31 (2011)
2. Buckingham, R., Graham, A.: Dexterous manipulators for nuclear inspection and maintenance—case study. In: 2010 1st International Conference on Applied Robotics for the Power Industry, pp. 1–6. IEEE (2010)
3. Li, T., Ma, S., Li, B., Wang, M., Wang, Y.: Axiomatic design method to design a screw drive in-pipe robot passing through varied curved pipes. *Sci. China Technol. Sci.* **59**(2), 191–202 (2016)
4. Peng, J., Xu, W., Liu, T., Yuan, H., Liang, B.: End-effector pose and arm-shape synchronous planning methods of a hyper-redundant manipulator for spacecraft repairing. *Mech. Mach. Theory* **155**, 104062 (2021)
5. Wang, Y., Yang, G., Zheng, T., Yang, K., Lau, D.: Force-closure workspace analysis for modular cable-driven manipulators with co-shared driving cables. In: 13th IEEE Conference on Industrial Electronics and Applications (ICIEA), pp. 1504–1509. IEEE (2018)
6. Sanjeevi, N., Vashista, V.: Stiffness modulation of a cable-driven serial-chain manipulator via cable routing alteration. *J. Mech. Robot.* **15**(2), 021009 (2022)
7. Rezazadeh, S., Behzadipour, S.: Tensionability conditions of a multi-body system driven by cables. In: ASME International Mechanical Engineering Congress and Exposition, vol. 43033, pp. 1369–1375 (2007)
8. Ramadoss, V., Lau, D., Zlatanov, D., Zoppi, M.: Analysis of planar multi-link cable driven robots using internal routing scheme. In: International Design Engineering Technical Conferences and Computers and Information in Engineering Conference, vol. 83990. American Society of Mechanical Engineers, V010T10A029 (2020)
9. Wang, Y., Yang, G., Zheng, T., Shen, W., Fang, Z., Zhang, C.: Tension reduction method for a modular cable-driven robotic arm with co-shared cables. *Intell. Serv. Robot.* **15**(1), 27–38 (2022)
10. Sanjeevi, N., Vashista, V.: Effect of cable co-sharing on the workspace of a cable-driven serial chain manipulator. In: Proceedings of the Advances in Robotics 2019, pp. 1–6 (2019)
11. Rodriguez, S., Tang, X., Lien, J.-M., Amato, N.M.: An obstacle-based rapidly-exploring random tree. In: Proceedings 2006 IEEE International Conference on Robotics and Automation, ICRA 2006, pp. 895–900. IEEE (2006)
12. Guo, Y., Lau, D.: Heuristic-based design framework for the cable arrangement of cable-driven parallel robots. In: Gouttefarde, M., Bruckmann, T., Pott, A. (eds.) *CableCon 2021*. MMS, vol. 104, pp. 194–205. Springer, Cham (2021). https://doi.org/10.1007/978-3-030-75789-2_16